A NEW GLOBAL GAS HYDRATE BUDGET BASED ON NUMERICAL REACTION-TRANSPORT MODELING AND A NOVEL PARAMETERIZATION OF HOLOCENE AND QUATERNARY SEDIMENTATION

E. B. Burwicz[*]
L. H. Rüpke
K. Wallmann
Leibniz-Institut für Meereswissenschaften (IFM-GEOMAR)
Wischhofstrasse 1-3, 24148 Kiel,
GERMANY

ABSTRACT

This study provides new estimates for the global methane hydrate inventory based on reaction-transport modeling [1]. A multi-1D model for POC degradation, gas hydrate formation and dissolution is presented. The model contains an open three-phase system of two solid (organic carbon, gas hydrates), three dissolved (methane, sulfates, inorganic carbon) and one gaseous (free methane) compounds. The reaction module builds upon the kinetic model of POC degradation [2] which considers a down-core decrease in reactivity of organic matter and the inhibition of methane production via accumulation of metabolites in sediment pore fluids.

Global input grids have been compiled from a variety of oceanographic, geological and geophysical data sets including a parameterization of sedimentation rates in terms of water depth (Holocene) and distance to continents (Quaternary).The world's total gas hydrate inventory is estimated at 1.74×10^{13} m^3 – $\sim 2 \times 10^{15}$ m^3 CH$_4$ (STP) or, equivalently, 8.3 – $\sim$900 Gt of methane carbon. The first value refers to the present day conditions using the relatively low Holocene sedimentation rates; the second value corresponds to a scenario of higher Quaternary sedimentation rates along continental margins. This increase in the POC input could be explained by re-deposition process at the continental rise and slope due to erosion of continental shelf sediments during glacial times.

Our results show that in-situ POC degradation is at present not an efficient hydrate forming process. Significant hydrate deposits are more likely to have formed at times of higher sedimentation during the Quaternary or/and as a consequence of active upward fluid transport.

Keywords: gas hydrates, global budget, numerical modeling, reaction-transport model

[*] Corresponding author: phone: +49 (0)431 600 2866, e-mail: eburwicz@ifm-geomar.de

NOMENCLATURE

a_0 initial age of organic matter degradation [yr]

B basement depth [cm]

c_0 compaction length scale [= $0.83 \ 10^{-5}$ cm^{-1}]

c_1 fitting parameter [=3]

c_2 fitting parameter [=10]

$C(CH_4)$ concentration of dissolved methane [mM]

$C(DIC)$ concentration of dissolved inorganic carbon [mM]

$C(SO_4)$ concentration of dissolved sulfates [mM]

d_s density of dry sediments [=2.65 g cm^{-3}]

D_s diffusion coefficient [cm^2 yr^{-1}]

$G(POC)$ concentration of solid organic carbon [wt. %]

k_{AOM} kinetic constant [=10^{-8} mM^{-1} yr^{-1}]

K_C Monod inhibition constant [mM]

K_{SO4} kinetic constant [=1 mM]

k_x age dependent kinetic constant [yr^{-1}]

MW_C molecular weight of carbon [=12 g mol^{-1}]

n number of grid points [=300]

R_{AOM} kinetic rate of anaerobic methane oxidation [mM yr^{-1}]

r_C unit conversion factor (wt. % into mM)

R_M kinetic rate of methanogenesis [mM yr^{-1}]

R_{POC} kinetic rate of POC degradation [wt. % yr^{-1}]

R_{SR} kinetic rate of sulfate reduction [mM yr^{-1}]

T_o tortuosity

t time [yr]

w_0 burial velocity at the upper boundary [cm yr^{-1}]

w_1 fitting parameter [=0.117 cm yr^{-1}]

w_2 fitting parameter [=0.006 cm yr^{-1}]

z_0 seafloor depth [cm]

z_1 fitting parameter [=200 m]

z_2 fitting parameter [=4000 m]

z depth [cm]

κ thermal conductivity [=1.5 W m^{-1} K^{-1}]

λ characteristic depth [=$1/c_0$ cm]

υ velocity of dissolved species [cm yr^{-1}]

Φ_0 initial porosity at the seafloor [=0.7]

Φ porosity

w burial velocity of solid species [cm yr^{-1}]

INTRODUCTION

Gas hydrates are solid ice-like crystalline compounds in which hydrocarbon molecules are trapped within cages of host water molecules. Guest molecules include also higher hydrocarbons but methane is the most common one, which makes marine hydrates a potential energy resource and an important reservoir in the global carbon cycle.

In marine settings, gas hydrates are known to occur along passive and active continental margins where the physical conditions and organic carbon input favor their formation. In fact, hydrates are only stable at high pressure and low temperature conditions and a sharp phase boundary separates them from the free gas phase situated below. Hydrates are thus vulnerable to regional and global changes in sea level and temperature.

Quantifying the role of marine hydrates in the Earth System requires global estimates on their distribution and abundance. This has resulted in a rapidly increasing number of publications exploring the various aspects of their formation [3]. On a regional scale, numerical modeling is complementing a wealth of observational studies and progressively helps to understand hydrate formation and dissolution processes in important gas hydrate provinces, i.e. Hydrate Ridge, offshore Oregon [4-7]. Global predictions rely on numerical modeling [8-10] and region-by-region extrapolation (i.e. adequate for passive and active margins) of the total amount of hydrate-bearing marine sediments and locally inferred fraction of hydrates [3, 11]. Recently published estimates on the global carbon inventory locked up in offshore hydrates vary over several orders of magnitude from 500 to 57 000 Gt C [3, 8-11]. There is clearly an urgent need to better constrain these global estimates to evaluate both the resource potential and the contribution of hydrates to past and future climate change.

The aim of this study is to constrain the global inventory of methane hydrates in the seabed formed by the microbial degradation of organic matter within the GHSZ. For this purpose we have recently applied transport-reaction model that resolves for in-situ particular organic carbon (POC) degradation and hydrate formation and apply the model globally in a multi-1D mode [1]. In contrast to previous attempts [8-10, 12], the new model considers the down-core decrease in reactivity of organic matter [2, 13]. A validation of this approach was presented in the original Wallmann's paper [2] (Sea of Okhotsk and Blake Ridge) and in the paper by Marquardt for a wide range of ODP sites (Costa Rica, Peru, Chile, California, Blake Ridge, and Namibia) [14].

GLOBAL INPUT DATA

Input data sets have been compiled from variety of different sources and used in the model as global data maps with 1° × 1° resolution. To obtain the

correct thickness of gas hydrate stability zone (GHSZ) we have extracted the global bathymetry, bottom water temperature, and salinity data sets from an Ocean General Circulation Model (OGCM) simulation run in the ORCA_R025 configuration [15] which were originally performed on a tri-polar mesh (lateral resolution $0.25° \times 0.25°$ and vertical resolution 6-250 m). Global heat flow data set has been used as a proxy to geothermal gradients (provided by the International Heat Flow Commission (IHFC) [16]. Thermal conductivity was assumed to be constant ($\kappa = 1.5$ W m^{-1} K^{-1}). This assumption is based on the simple calculation of the averaged pore water and matrix conductivities for a shaly-sandstone lithology.

Global sediment thickness data have been combined from two data sets- NOAA data [17] and arctic region data [18].

According to the data from [19] and [20] we have compiled a global accumulation rate of particulate organic carbon (POC) in marine surface sediments which is the key parameter controlling gas hydrate formation.

Holocene sedimentation rates were calculated according to Eq. 1 which assumes that the burial velocity of Holocene surface sediments decreases with increasing water depth.

$$w = \frac{w_1}{1+\left(\dfrac{z}{z_1}\right)^{c1}} + \frac{w_2}{1+\left(\dfrac{z}{z_2}\right)^{c2}} \qquad (1)$$

However, some direct observations of the GHSZ thickness show that the depth of Holocene sediments is smaller than the gas hydrate presence zone. This suggests that there is a clear need to constrain more appropriate estimates on the rates of sedimentation averaged over a period of several million years.

It is well known that gas hydrate accumulations occur at the water depths larger than 300-350 m.

As it was suggested by [21] the Holocene sedimentation occurring at the continental shelves were shifted during the glacial conditions to the larger water depths (200-3000 m). Moreover, the transport of ice-rafted material and the deposition of eolian dust were strongly enhanced further increasing the accumulation rates at the margin seafloor [22].
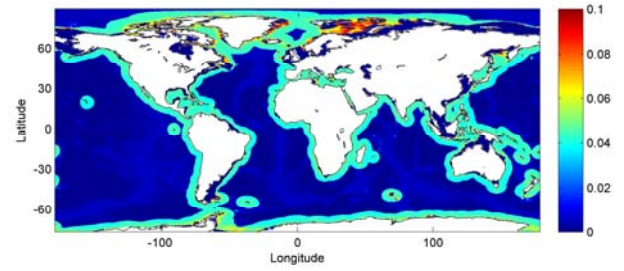

Fig. 1. Quaternary sedimentation rates used as an input in the second scenario of hydrate formation.

To explore this scenario we have run our hydrate accumulation model using an increased sedimentation rates at the continental slopes. We have provided two different calculations of potential gas hydrate accumulation due to in-situ POC degradation. First scenario assumes relatively low Holocene sedimentation rates which results in a minimum estimate of marine hydrate accumulations at the continental slope and rise. Second scenario accounts for the hydrate formation under Quaternary boundary conditions (see Fig. 1). In this case the rates of sedimentation at the distance from continents <500 km were increased by moving the material deposited at shallow water depths (up to 200 m) to the continental slopes. The total amount of sediments remains the same over the global ocean area.

NUMERICAL MODEL
Introduction

We have developed a multi-1-D numerical model of gas hydrate formation and dissolution processes in anoxic marine sediments. The reaction-transport model contains various chemical compounds (solid organic carbon, dissolved in pore water methane, dissolved inorganic carbon, dissolved sulfates, gas hydrates, and free methane gas). The rates of POC degradation, anaerobic methane oxidation, sulfate reduction, and methanogenesis are kinetically controlled. Concentration profiles were run until the steady-state. We did not account for the potential local salinity changes due to hydrate formation or dissolution processes. Gas hydrate stability zone (GHSZ) was defined as a combination of pressure, temperature, and (to a smaller degree) salinity conditions. The lower boundary of the GHSZ was attached to the intersection of gas hydrate and methane gas solubilities calculated according to the equations from [23].

Wherever the concentration of dissolved methane exceeds the critical saturation, gas hydrate formation occurs (similar process takes place for the free gas formation). Oversaturation was prevented by the kinetic constants of the gas hydrate and methane gas formation. Microbial and chemical reaction rates were updated after each time step.

The diffusion equations are solved using a fully-implicit finite-differences method, while all transport processes are resolved by a Semi-Lagrangian scheme. The entire model was implemented in Matlab 7.7.0 (R2008b).

Reference frame

We consider a reference frame which extends from the seafloor to the bottom of the GHSZ plus 50m of Free Gas Zone lying directly beneath. However, the upper part of sediment column (10 cm) was not considered in the model due to strong bioturbation processes which might potentially have an impact on the gradients of dissolved in pore fluids chemical species. This implies that the spatial location of the upper boundary is fixed and does not follow sediment burial which results in a net downward migration of deposited sediments. The length of each sediment column is constant over time and is limited according to the global sediment thickness data. Therefore, the model column does not include the Free Gas Zone for those cases where the thickness of the GHSZ exceeds the sediment thickness. This fixed lower boundary results in the advective loss of system components through the bottom of the modeling domain.

Porosity, which decreases exponentially with depth, is calculated using Eq. 2 from [24] for the initial porosity ϕ_0 and compaction length scale c_0. According to the reference frame, porosity remains constant at every grid point.

$$\phi(z) = \phi_0 \cdot \exp(c_0 \cdot z) \qquad (2)$$

Boundary and initial conditions

As boundary conditions we assume constant concentrations of dissolved methane, dissolved inorganic carbon, and sulfate on top of each modeled sediment column. Burial velocities at zero depth (w_0) were defined as a function of water depth (see Eq.1). In a second set of model runs, w_0 values were enhanced along continental margins to estimate Quaternary burial velocities.

Zero concentration gradients were applied at the lower boundary of the model column.

At modeling time zero sediment pore space was filled by pore fluids with salinity values consistent with the one at the sediment-water interface. The initial concentrations in the uppermost segment of the model column were defined according to the upper boundary conditions. Within the sediment column, the initial concentrations of POC, dissolved CH_4 and DIC were set to zero while a simple exponential function was applied to define the down-core decrease in initial dissolved sulfate concentrations. Pressure regimes were calculated separately for each sediment bin as hydrostatic pressure values considering ambient water and sediment depths. Temperature profiles are set according to the bottom water temperature and heat flow data.

Compaction and advection velocities

Sedimentation and compaction processes imply, in the chosen reference frame, a continuous downward movement of sediment grains with respect to the seafloor (Eq. 3):

$$w(z) = \frac{-w_0(1-\phi_0)}{(1-\phi)} \qquad (3)$$

Sediment compaction results in pressurization and expulsion of pore fluids carrying dissolved chemical species. In high permeability systems all excess pressures are released by relative upward flow; significant excess pressures can build up in systems of low permeability. Permeability is often correlated to porosity and may further be affected by hydrate content. It was reported that the size of sediment pores may affect the process of gas hydrate formation [4]. Lithology of potential hydrate-bearing zone (i.e. coarse-grained sands) may result in preferential hydrate accumulation. According to Darcy's law, high permeability allows for enhanced gas fluxes. However, a buffer effect caused by decreasing effective porosity due to formation of thick hydrate layers close to the bottom of the Gas Hydrate Stability Zone may block the advective free gas transport and support further hydrate accumulation within the lower part of GHSZ. These mechanisms are still poorly understood and were, thus, not considered in our model. Here we assume that permeability is always sufficiently high for pore fluids to be expelled by compaction. This allows us to use an

analytical expression (Eq. 4) for pore fluid flow [25]:

$$\upsilon(z) = \frac{-w_0(1-\phi_0)\cdot\exp{(z-B/\lambda)}}{1-\phi_0\cdot\exp{(-B/\lambda)}} \quad\quad (4)$$

Basement of each sediment column (B) from the fluid velocity equation was set to a value adequate for depths where porosity reaches the level of 20 % and thus, compaction processes become negligible. Note that this equation solves for fluid flow with respect to the seafloor and flow is therefore always directed downwards but of lower magnitude than the solid velocity. A potential gas phase included in the model is buried with sediment grains using the solid velocity.

Governing equations for solid and dissolved compounds
Two major phases essential for gas hydrate formation were considered: pore fluids containing dissolved chemical species (CH_4, DIC and SO_4) and solids including incompressible sediment grains and particulate organic carbon. Free gas (formed due to hydrate recycling processes at the bottom of GHSZ or directly by POC degradation at great depths below the GHSZ) is attached to sediment grains and transported downward with solid phase velocity. Upward gas advection is thus neglected in the model since measurements in consolidated sediments indicate that gas migration occurs only if more than approximately 10 % of the pore space is occupied by gas [4].

Transport of solid as well as dissolved compounds were solved as an advection process occurring via sediment burial into great depths with solid (w) and fluid (υ) velocities. Source terms contain time and depth-dependent rates of various chemical reactions (organic carbon decay, anaerobic oxidation of methane, methanogenesis, and sulfate reduction). Advection and diffusion processes have been split and solved separately for each component.

Equation 5 describes mass conservation of solid species. The first term on the right-hand side represents the advective transport of solid compounds, while the second term accounts for all chemical reactions.

$$(1-\phi)\cdot\frac{\partial G}{\partial t} = -\frac{\partial((1-\phi)\cdot w\cdot G)}{\partial z} + (1-\phi)\cdot R \quad (5)$$

Mass conservation of dissolved species is defined by Eq. 6 in which the first term on the right-hand side describes advective transport with the fluid velocity, the second one accounts for the molecular diffusion of dissolved species, and the last (source) term represents chemical reactions.

$$\phi\cdot\frac{\partial C}{\partial t} = -\frac{\partial(\phi\cdot\upsilon\cdot C)}{\partial z} + \frac{\partial(\phi\cdot D_s\cdot\frac{\partial C}{\partial z})}{\partial z} + \phi\cdot R \quad\quad (6)$$

Molecular diffusion of dissolved species through the entire sediment profile is controlled by changes in concentration gradients. Diffusion coefficients of dissolved chemical compounds in sediments are calculated as molecular diffusion coefficients (D_m) for constant temperature (2°C) and salinity (35 PSU) according to the equations from [26] and scaled by tortuosity (T_o) from [27] (Eq. 7).

$$T_0{}^2 = 1 - 2\cdot\ln(\phi) \quad\quad (7)$$

Diffusion coefficient of dissolved inorganic carbon was treated as a combination of HCO_3^- and CO_2 diffusivity which are the most wide-spread inorganic carbon carriers within marine anoxic sediments in close to neutral pH regimes.

Source terms
A key reaction is the degradation of organic matter (POC) which follows the kinetic approach developed by Wallmann [2]. This kinetic equation considers the decrease in organic matter reactivity with depth and age of sediments [13] and the inhibition of anaerobic degradation processes by the accumulation of dissolved metabolites in ambient pore fluids. Monod constant K_c describes the inhibition of organic matter decomposition by the concentration of CH_4 and DIC. High values of K_c constant favor rapid POC decomposition and, consequently, gas hydrate formation.

A comparison of the new rate law with the classic Middelburg formulation showed that in mainly anoxic sediments with high concentrations of metabolites, Wallmann's kinetic equation results in diminished POC degradation rates that are in good agreement with pore water data obtained at ODP site 997 (Blake Ridge) and seven stations at Sakhalin slope (Sea of Okhotsk) [2]. Subsequently, the Wallmann formulation was applied to a wide range of geological settings represented by ODP sites 1041 (Costa Rica), 685 and 1230 (Peru), 1233 (Chile), 1014 (California), 995 (Blake Ridge), and 1084 (Namibia) [14].

Required modeling parameters were taken directly from ODP reports and a good fit to the observed concentrations of dissolved metabolites accumulating in the pore fluids of the studied sediments was obtained applying a K_c value of 25 to 50 mM. Here, we used a relatively high value of 47 mM to allow for significant gas hydrate formation from in-situ POC degradation. Since microbial formation of methane remains only one of the multiple gas sources in marine sediments, our results should be considered as the minimum estimate of offshore gas hydrate deposits. The age-dependent kinetic constant k_x was computed following a simple formulation assuming a depth-decreasing reactivity of metabolites ([13]; see Tab. 1).

Tab. 1. Kinetic rate laws used in the model

Rate	Formulation
R_{POC}	$\dfrac{K_c}{C(DIC)+C(CH_4)+K_c} \cdot k_x \cdot G(POC)$
R_{AOM}	$k_{AOM} \cdot C(SO_4) \cdot C(CH_4)$
R_M	$0.5 \cdot \dfrac{K_{SO_4}}{C(SO_4)+K_{SO_4}} \cdot R_{POC} \cdot r_C$
R_{SR}	$0.5 \cdot \dfrac{C(SO_4)}{C(SO_4)+K_{SO_4}} \cdot R_{POC} \cdot r_C$
k_x	$0.16 \cdot \left(a_0 + \dfrac{z}{w}\right)^{-0.95}$
r_C	$\dfrac{\phi \cdot MW_C}{(1-\phi) \cdot d_s \cdot 10^4}$

The upper boundary of each modeling domain is situated 10 cm below the real sediment surface where the effects of bioturbation and bioirrigation processes become negligible. Thus, the initial age of POC degradation from represents time needed to reach the undisturbed sediments.

POC is degraded via microbial sulfate reduction until the dissolved sulfate pool in ambient pore waters is depleted. Below the sulfate penetration depth, POC is microbially decomposed into methane and CO_2. Upward diffusing dissolved methane is consumed by anaerobic oxidation within the sulfate-methane transition zone. The rate of anaerobic oxidation of methane (R_{AOM}) depends on methane and sulfate concentrations in pore fluids and is additionally controlled by the kinetic constant k_{AOM}.

RESULTS AND DISCUSSION

We have analyzed two scenarios of low and high sedimentation which represent minimum and maximum estimates of hydrate accumulation via microbial methane formation.

In the low sedimentation rate scenario we explored the dynamics of hydrate formation under Holocene boundary conditions. The total amount of methane carbon from hydrates is estimated to be ~8.3 Gt. Gas hydrate deposits are distributed mostly in the Central America and Arctic region with concentrations not exceeding 150 kg C m^{-2}. Our results show that widespread hydrate formation based on in-situ POC degradation is very unlikely to occur due to low burial velocities of particulate organic matter. The amount of dissolved methane is usually too small to exceed the CH_4 solubility curve which is the critical step for hydrate precipitation. This model result clearly shows that hydrate formation is severely limited by low sedimentation rates at the continental slope and rise. Trapping of terrigenous particles in the shelf environment, thus, effectively inhibits hydrate formation via microbial POC degradation within the GHSZ under Holocene boundary conditions.

The Quaternary sedimentation conditions applied in the second scenario result in significant and wide-spread gas hydrate accumulations along active and passive continental margins (i.e. western and eastern coasts of North and South America). Hydrates are also formed in parts of the Indian Ocean, the Arctic Ocean, the Southern Ocean and the equatorial Pacific.

Total amount of methane gas trapped within hydrate-bearing sediments in the high sedimentation scenario is estimated at ~2 x 10^{15} m^3 (expanded to atmospheric conditions) or, equivalently, ~900 Gt of methane carbon (see Tab. 2).

Tab. 2. Gas hydrate accumulations under Quaternary boundary conditions

Distance to continents	Total area covered by margins	Total amount of gas hydrates
400 km	89.347 million km^2	959 Gt C
500 km	106.70 million km^2	819 Gt C
Holocene boundary conditions		8.3 Gt C

These values are in good agreement with predictions of 500-2500 Gt of carbon presented by Milkov [3] based on field observations.

The highest gas hydrate concentrations (up to 830 kg of carbon m^{-2}) are observed in regions of high organic carbon accumulation, i.e. Central America, eastern coast of South America, Laptev Sea, and Arabian Sea and do not correlate in a simple way with GHSZ thicknesses. For up to 0.5 % of the total number of hydrate-bearing modeling domains

gas hydrate concentrations exceed 400 kg C m^{-2} (i.e. Central America, Arctic, and Arabian Sea). Gas hydrates have been previously documented at various cold seeps [28] and ODP sites along the central American margin [29]. Moderate hydrate concentrations (150-400 kg C m^{-2}) occur at ~8.5 % of total hydrate provinces (western and eastern coasts of North America, Arctic, Sea of Okhotsk, Antarctic, eastern coast of Australia, Africa continental margin, Indian Ocean, Central America, and eastern coast of Greenland). The remaining regions of hydrate accumulation feature low hydrate saturations (<150 kg C m^{-2}).

Rich hydrate deposits in the Arctic are stabilized by relatively low bottom water temperatures. However, shallow hydrate accumulations in the Arctic are more vulnerable to temperature and sea level changes and could produce significant amounts of dissolved or gaseous methane [30].

Previous global estimates of marine gas hydrates were presented by Buffett and Archer [9]. This hydrate inventory of 3000 Gt C was to a large degree controlled by the velocity of upward fluid flow that was assumed to exceed the flow rate induced by sediment compaction by 20 % (passive margins) to 60 % (active margins). Without imposed fluid flow, the global hydrate inventory was reduced to 600 Gt C [9] and further to 700 – 900 Gt C [8].

In contrast to the study of Buffett and Archer [9] and the one presented in this paper, the numerical approach of Klauda and Sandler [10] results in relatively large global hydrate inventory of ~57 000 Gt C. They assume the complete degradation of the entire POC pool with a reduced decay constant of 1.5×10^{-14} s^{-1} and no organic matter degradation via sulfate reduction processes. Thus, efficient methane production in the upper part of the sediment column is not inhibited by the presence of dissolved sulfate. The Klauda and Sandler model was run without imposing upward fluid flow.

This large difference may be explained by the neglect of microbial sulfate reduction and AOM since the accumulation of methane in pore fluids and gas hydrates is strongly diminished by these processes. Moreover, Buffett and Archer and Klauda and Sandler applied the thermodynamic equilibrium model between gas hydrate, sea water, and methane gas phases presented by Zatsepina and Buffett [31], whereas our model is based on the study presented by Tishchenko [23]. The latter approach considers the measured CH$_4$ solubility in seawater and is in good agreement with other published data [32].

Comparatively, the world's conventional gas endowment which is estimated at 2.567 TBOE (Trillion Barrels of Oil Equivalent) equivalent to 436.4×10^{12} m^3 of natural gas [33], is at least a few times smaller than the global methane hydrate inventory calculated in our Quaternary simulation. It should, however, be noted that the simulation results and the global inventories presented in this study are only valid for finely dispersed gas hydrates.

The availability of organic carbon at the seafloor is thought to be one of the most essential parameters limiting gas hydrate formation [10, 34, 35]. The minimum concentration of TOC necessary to initiate and sustain hydrate precipitation was suggested to be larger than 1 wt. % [35], 0.5 wt. % [34]. We suggest that hydrate formation is not controlled by concentration of organic carbon but rather by the combination of TOC concentration and sedimentation rate.

The minimum amount of TOC needed to form gas hydrates oscillates around 0.3 wt. % for high sedimentation rates and relatively shallow water depths (~250 m). This threshold value increases with decreasing sedimentation rate and reaches a value of >1.0 wt. % at low sedimentation rates (~1 cm kyr^{-1}) characteristic for large water depths and open ocean settings. The concentration threshold for hydrate formation is thus not a fixed value but a function of sedimentation rate.

CONCLUSIONS

Using our approach the world's total inventory of gas hydrates is estimated at 1.74×10^{13} m^3 – ~2 x 10^{15} m^3 CH$_4$ (STP) or, equivalently, 8.3 – ~900 Gt of methane carbon [1]. The low estimate corresponds to the Holocene sedimentation scenario, while the high estimate refers to a scenario of higher Quaternary sedimentation at continental slope and rise settings. These estimates are significantly lower than previously reported and are based on improved reaction kinetics of POC degradation and a new compilation of global input data.

The new estimate of Holocene sedimentation rates presented in this contribution clearly shows that widespread gas hydrate formation is very unlikely to occur under Holocene boundary conditions.

It appears likely that active upward transport of free methane gas and methane rich pore fluids from underlying sediment sequences is the main driving force of hydrate formation during the Holocene.

The high sedimentation scenario is likely to represent the present, steady-state hydrate budget formed in-situ by organic matter degradation. It considers that hydrate formation is occurring over the entire GHSZ with includes sediments deposited not only during the Holocene but rather over a time span of several million years. Relatively high rates of sedimentation during the glacial periods of the Quaternary provided gas hydrate formation within continental margins thereby increasing the global budget of hydrates.

It should be noted that the hydrate accumulations presented in this study do not include hydrate deposits formed by the focused ascent of gas and fluids from deeper sedimentary strata. It is presently not possible to estimate the global amount of these additional hydrate deposits. Regional geophysical surveys and drilling information is needed to better constrain the abundance of these economically very promising deposits.

REFERENCES

[1] Burwicz E. B., Rüpke L. H., and Wallmann K., *Estimation of the global amount of submarine gas hydrates formed via microbial methane formation based on numerical reaction-transport modeling and a novel parameterization of Holocene sedimentation (under review).* Geochimica et Cosmochimica Acta, 2011.

[2] Wallmann K., et al., *Kinetics of organic matter degradation, microbial methane generation, and gas hydrate formation in anoxic marine sediments.* Geochimica et Cosmochimica Acta, 2006. **70**: p. 3905 - 3927.

[3] Milkov A. V., *Global estimates of hydrate-bound gas in marine sediments: how much is really out there?* Earth-Science Reviews, 2004. **66**: p. 183 - 197.

[4] Garg S. K., et al., *A mathematical model for the formation and dissociation of methane hydrates in the marine environment.* Journal of Geophysical Research, 2008. **113**.

[5] Liu X. and Flemings P. B., *Passing gas through the hydrate stability zone at southern Hydrate Ridge, offshore Oregon.* Earth and Planetary Science Letters, 2006. **241**: p. 211 - 226.

[6] Luff R. and Wallmann K., *Fluid flow, methane fluxes, carbonate precipitation and biogeochemical turnover in gas hydrate-bearing sediments at Hydrate Ridge, Cascadia Margin: Numerical modeling and mass balances.* Geochimica et Cosmochimica Acta, 2003. **67**(18): p. 3403 - 3421.

[7] Torres M. E., et al., *Gas hydrate growth, methane transport, and chloride enrichment at the southern summit of Hydrate Ridge, Cascadia margin off Oregon.* Earth and Planetary Science Letters, 2004. **226**: p. 225 - 241.

[8] Archer D., Buffett B., and Brovkin V., *Ocean methane hydrates as a slow tipping point in the global carbon cycle.* Proceedings of the National Academy of Sciences, 2008. **106**(49): p. 20596 - 20601.

[9] Buffett B. and Archer D., *Global inventory of methane clathrate: Sensitivity to changes in the deep ocean.* Earth and Planetary Science Letters, 2004. **227**: p. 185 - 199.

[10] Klauda J. B. and Sandler S. I., *Global Distribution of Methane Hydrate in Ocean Sediment.* Energy & Fuels, 2005. **19**: p. 459 - 470.

[11] Kvenvolden K. A. and Lorenson T. D., *A Global Inventory of Natural Gas Hydrate Occurrence.* USGS, Western Region Coastal and Marine Geology, 2001. **201**.

[12] Archer D. and Buffett B. A., *Time-depended response of the global ocean clathrate reservoir to climatic and anthropogenic forcing.* Geochemistry, Geophysics, Geosystems, 2005. **6**(3).

[13] Middelburg J. J., *A simple rate model for organic matter decomposition in marine sediments.* Geochimica et Cosmochimica Acta, 1989. **53**: p. 1577 - 1581.

[14] Marquardt M., et al., *A transfer function for the prediction of gas hydrate inventories in marine sediments.* Biogeosciences, 2010. **7**(9): p. 2925 - 2941.

[15] Barnier B., *Impact of partial steps and momentum advection schemes in a global ocean circulation model at eddy-permitting resolution.* Ocean Dynamics, 2006. **56**: p. 543 - 567.

[16] Hamza V. M., Cardoso R. R., and Ponte Neto C. F., *Spheical harmonic analysis of earth's conductive heat flow.* International Journal of Earth Sciences (Geol Rundsch), 2008. **97**: p. 205 - 226.

[17] Divins D. L., *Total Sediment Thickness of the World's Oceans & Marginal Seas.* 2003, NOAA National Geophysical Data Center (NGDC).

[18] Laske G. and Masters G., *A Global Digital Map of Sediment Thickness*. 1997, American Geophysical Union.

[19] Seiter K., et al., *Organic carbon content in surface sediments- defining regional provinces.* Deep-Sea Research I, 2004. **51**: p. 2001 - 2026.

[20] Romankevich E. A., Vetrov A. A., and Peresypkin V. I., *Organic matter of the World Ocean.* Russian Geology and Geophysics, 2009. **50**: p. 299 - 307.

[21] Hay W. W., *Pleistocene-Holocene Fluxes Are Not the Earth's Norm*, in *Material Fluxes on the Surface of the Earth*, Hay W. W. and Usselman T., Editors. 1994, National Academy Press: Washington. p. 15 - 27.

[22] Lisitzin A. P., *Oceanic Sedimentation: Lithology and Geochemistry*. 1996, Washington, D. C.: American Geophysical Union. 400.

[23] Tishchenko P., et al., *Calculation of the stability and solubility of methane hydrate in seawater.* Chemical Geology, 2005. **219**: p. 37 - 52.

[24] Athy L. F., *Density, porosity, and compaction of sedimentary rocks.* AAPG Bulletin, 1930. **14**: p. 1 - 24.

[25] Hutchison I., *The effects of sedimentation and compaction on oceanic heat flow.* Geophysical Journal of the Royal Astronomical Society, 1985. **82**: p. 439 - 459.

[26] Boudreau B. P., *Diagenetic Models and Their Implementation: Modelling Transport and Reactions in Aquatic Sediments*. 1997, Berlin, New York: Springer-Verlag.

[27] Boudreau B. P., *The diffusive tortuosity of fine-grained unlithified sediments.* Geochimica et Cosmochimica Acta, 1996. **60**(16): p. 3139 - 3142.

[28] Schmidt, M., et al., *Methane hydrate accumulation in "Mound 11" mud volcano, Costa Rica forearc.* Marine Geology, 2005. **216**: p. 83-100.

[29] Hensen, C. and K. Wallmann, *Methane formation at Costa Rica continental margin - constraints for gas hydrate inventories and cross-décollement fluid flow.* Earth and Planetary Science Letters, 2005. **236**: p. 41-60.

[30] Reagan M. T. and Moridis G. J., *Dynamic response of oceanic hydrate deposits to ocean temperature change.* Journal of Geophysical Research, 2008. **113**(C12023).

[31] Zatsepina O. Ye. and Buffett B. A., *Thermodynamic conditions for the stability of gas hydrate in the seafloor.* Journal of Geophysical Research, 1998. **103**: p. 24 127 - 24 139.

[32] Duan Z., Moller N., and Weare J. H., *An equation of state for the CH_4-CO_2-H_2O system: I. Pure systems from 0 to 1000 ^{o}C and 0 to 8000 bar.* Geochimica et Cosmochimica Acta, 1992. **56**: p. 2605 - 2617.

[33] USGS World Energy Assessment Team, *U.S. Geological Survey World Petroleum Assessment 2000-- description and results*. 2000.

[34] Revelle R. R., *Methane Hydrates in Continental Slope Sediments and Increasing Atmospheric Carbon Dioxide. In:* , in *Changing Climate*. 1983, Report of the Carbon Dioxide Assessment Committee: National Academic Press, Washington, DC. p. 252.

[35] Kvenvolden K. A., *Methane hydrate - A major reservoir of carbon in the shallow geosphere?* Chemical Geology, 1988. **71**(1 - 3): p. 41 - 51.